Journal of Visualization, Vol. 11, No. 1 (2008) 3

Portfolio Paper

Grain Sorting on Sand Ripples in Heterogeneous Sediments

Voropayev, S. I.*[1, 2], Balasubramanian, S.*[1] and Fernando, H. J. S.*[1]
*1 Arizona State University, Tempe, AZ 85287-9809, USA. E-mail: s.voropayev@asu.edu
*2 Institute of Oceanology, Russian Academy of Sciences, Moscow, 117851, Russia.
Received 26 April 2007 and Revised 6 July 2007

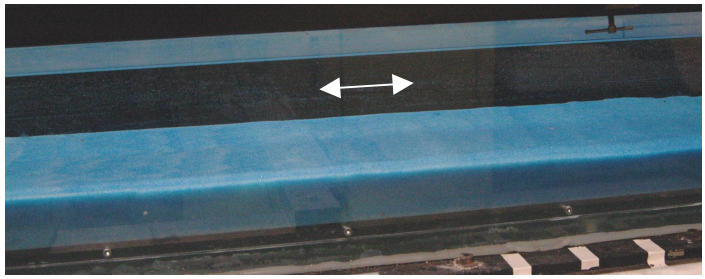

Fig. 1. Initially flat sand mixture (oblique view) in a water channel. Arrows show the oscillatory flow directions. Frame width is 100 cm.

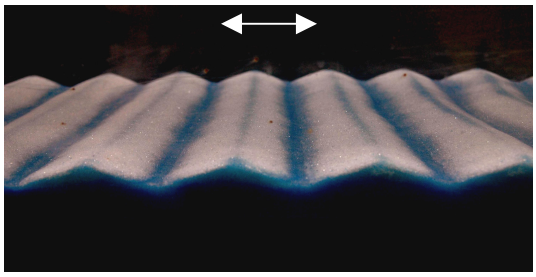

Fig. 2. Typical sediment segregation pattern in established ripples, side view. Fine grains (blue) are mostly seen on the ripple troughs with very narrow strips on the tops of the ripple crests; coarse grains (brown) are seen mostly on the ripple crests. Frame width is 45 cm.

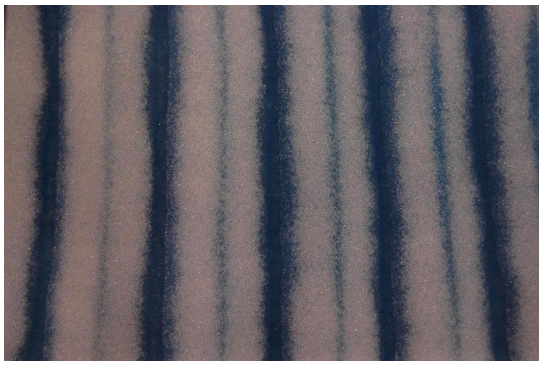

Fig. 3. As Fig. 2, but top view.

Sand ripples are commonly observed coastal benthic features that form under the action of waves/currents. In most previous studies of ripple dynamics homogeneous sand was used (see, e.g., Testik et al., 2005 and references herein)(1). In nature, sands are mostly heterogeneous. In the figures above we give an example of typical grain sorting as observed in a bimodal sand mixture under steady oscillatory flow in a water channel. The mixture consists of 34 % of fine sand (d = 0.3 mm, blue) and 66 % of course sand (d = 0.6 mm, brown). Initially flat (Fig. 1), sand mixture is subject to oscillatory flow (from left to right). With time, established ripples are formed (Figs. 2 and 3) with typical sediment segregation pattern: fine grains (blue) are mostly seen on the ripple troughs with very narrow strips on the tops of the crests; coarse grains (brown) are seen mostly on the ripple crests.

References: (1) Testik, F. Y. et al., Physics of Fluids, 17 (2005), 072104.

Journal of Visualization, Vol. 11, No. 1 (2008) 4

Portfolio Paper

Breakup Patterns for Binary Drop Collisions

Testik, F. Y.* and Young, D. M.*

* Dept. of Civil Engineering, College of Engr. and Sci., Clemson University, Clemson SC 29634, USA. E-mail: ftestik@clemson.edu

Received 7 August 2007 and Revised 22 October 2007

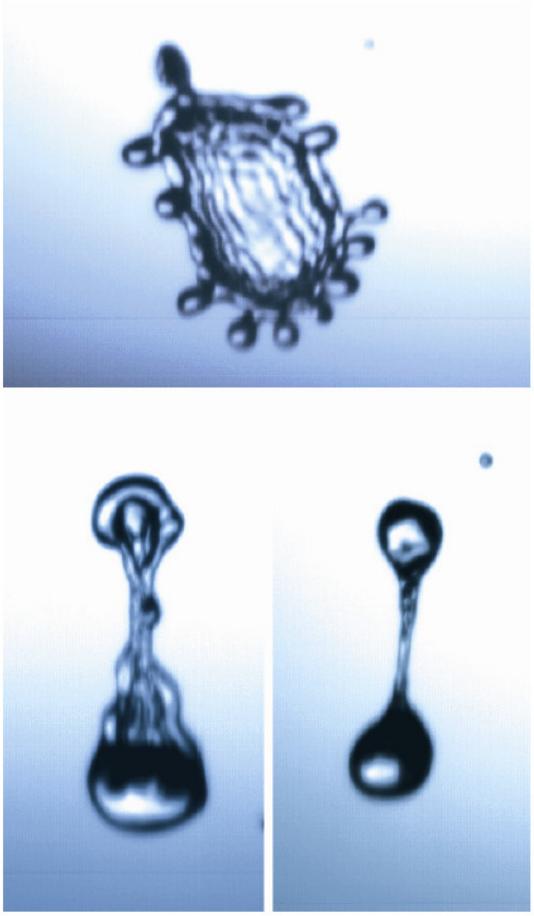

Fig. 1. Disk (top image), sheet (bottom-left image), and neck (bottom-right image) breakup patterns for binary drop collisions. In the experiments, drops are generated by the breakup of water jets formed by the flow of pressurized water through two hypodermic needles. These needles are oriented such that binary drop collisions are produced in the focal plane of a high-speed camera recording at 500 frames per second. The camera is pointed towards a light source and the drop collisions take place between the camera and the light source. The detailed description of this visualization technique is given by Testik et al. (2006) [(1)].

Colliding drops may breakup if sufficient energy is supplied to overcome the surface tension forces. There are three distinct breakup patterns primarily observed: disk, sheet, and neck breakups (Fig. 1; for details see Testik and Barros, 2007) [(2)]. In disk breakup, colliding drops temporarily coalesce and a disk of water begins to spread out from the point of impact. During this process, increased drag force acting on the disk-shaped water body causes a rapid deceleration. Once the disk reaches its maximum extent, the outer fringe sheds drops and then the entire disk gradually disintegrates into a relatively large number of fragments. In sheet breakup, the smaller of the colliding drops tears off one side of the larger drop. Subsequently, the bulk of the large drop starts rotating about the point of impact, while an extending film or sheet of water forms from the impact area. The small drop often disappears in this sheet and the large drop becomes strongly distorted. The disintegration of this sheet forms a number of fragments. In neck breakup, a water neck joining the two colliding drops forms due to a glancing contact. The smaller of the drops does not appear to affect the larger drop, except in the immediate vicinity of the point of contact. After separation, the large and small drops are still substantially intact, but fragments form as a result of the breakup of the neck.

References :. (1) Testik, F. Y. et al., Atmospheric Sciences, 63-10 (2006), 2663-2668. (2) Testik, F. Y. and Barros, A. P., Reviews of Geophysics, 45-2 (2007), Art No. RG2003.

Journal of Visualization, Vol. 11, No. 1 (2008) 5

Portfolio Paper

Visualization of Unsteady Viscous Flow around Turbine Blade

Jimbo, T.[*1], Biswas, D.[*1], Yokono, Y.[*1] and Niizeki, Y.[*2]

*1 Corporate Research and Development Center, Toshiba Corporation,1, Komukai-Toshiba-cho, Saiwai-ku, Kawasaki, Kanagawa, 212-8582, Japan. E-mail: tomohiko.jimbo@toshiba.co.jp

*2 Power and Industrial Systems Research and Development Center, Toshiba Corporation, 2-4, Suehiro-cho, Tsurumi-ku, Yokohama, Kanagawa, 230-0045, Japan.

Received 2 November 2007 and Revised 5 November 2007

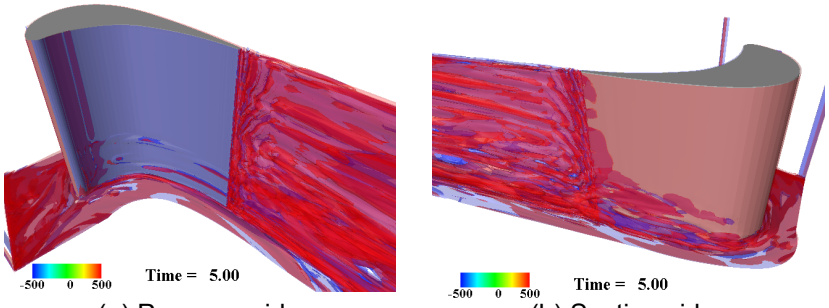

(a) Pressure side (b) Suction side

Fig. 1. Vorticity iso-surface (Incidence angle: 20 deg).

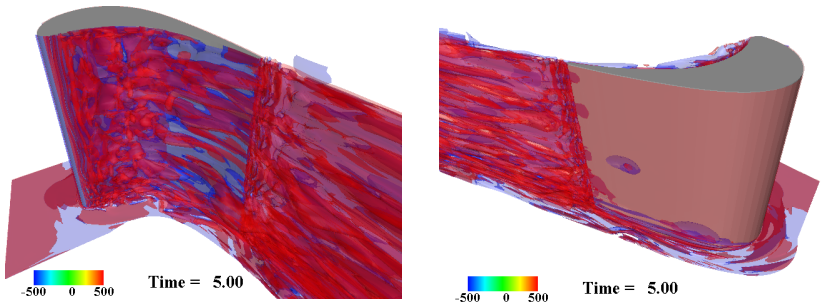

(a) Pressure side (b) Suction side

Fig. 2. Vorticity iso-surface (Incidence angle: 70 deg).

3-D unsteady viscous flow analysis around turbine blade cascade using Higher-order LES turbulent model(1) is carried out to investigate basic physical process involved in the pressure loss mechanism. Analysis simulated wind tunnel cascade test. The basic equations are unsteady 3-D continuity and momentum equations for incompressible flow and boundary conditions are as follows, wall boundaries are blade surface and hub surface. Single computation domain is used assuming that large number of blades with equal pitch is arranged in the pitch-wise direction and periodic boundary considerations are used in the span-wise direction.

In Fig. 1(a) and (b) are presented the results of 3-D computation on vorticity iso-surface(2) at the pressure side and suction side of turbine blade, respectively for flow incidence angle of 20 degree. Fig. 2(a) and (b) are those for flow incidence angle of 70 degree. Results presented in Fig. 1 and Fig. 2 indicate that in the wake region there occurs mixing between the clockwise vortex represented by blue color on the pressure side and anticlockwise vortex represented by red color on the suction side. In Fig. 1, secondary vortex formation at the hub wall can be observed. Flow is affected by secondary vortex and vortices at the wake region due to entrainment of fluid from the hub region, and pressure loss is increased. In Fig. 2, separation vortices are observed at the blade pressure side.

References : (1) Biswas, D., AIAA Paper, (2006), 2006-3684. (2) Yokono, Y. and Biswas, D., J. of Visualization, 10-3 (2007), 271-280.

Journal of Visualization, Vol. 11, No. 1 (2008) 6

Portfolio Paper

Schlieren Visualization of Vortices and Internal Waves Generated by Vertical Stroke Oscillations of a Disk

Chashechkin, Yuli D.* and Stepanova, E. V.*

* Institute for Problems in Mechanics of the Russian Academy of Sciences, 101/1 prospect Vernadskogo, Moscow, 119526, Russian Federation. E-mail: chakin@ipmnet.ru, and step@ipmnet.ru

Received 25 August 2007 and Revised 8 November 2007

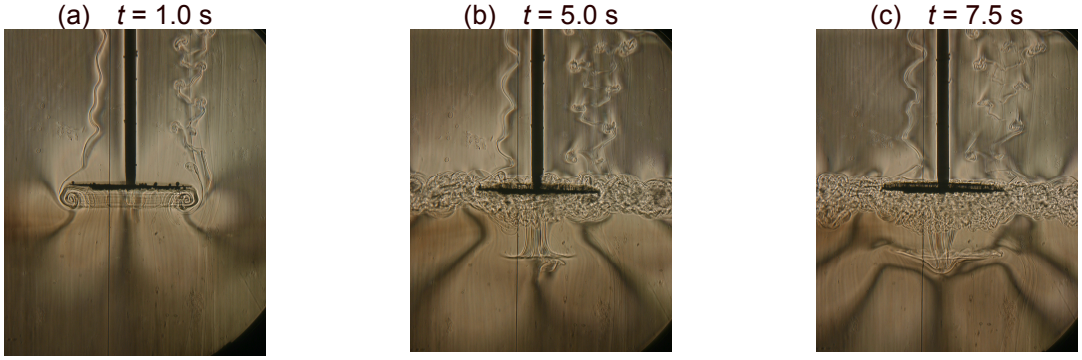

Fig. 1. Slit-thread schlieren images of flows induced by half-stroke of disk, T_b = 7.25 s, H = 3.1 cm.

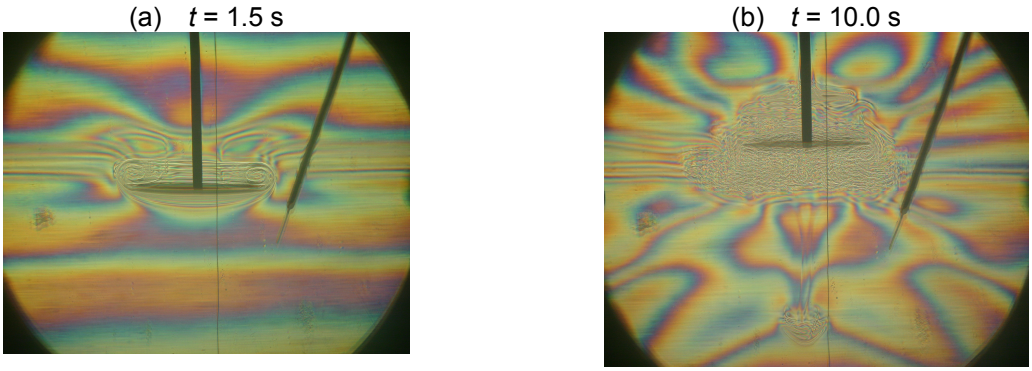

Fig. 2. "Natural rainbow" schlieren image of flow induced by stroke of disk, T_b = 11.2 s, H = 3.0 cm.

Side view of vortex flow induced by thin horizontal disk of diameter d = 6.4 cm performing vertical oscillations with double-amplitude peak H in a continuously stratified brine with the buoyancy period T_b s is shown. Used schlieren methodsP[(1)] are "slit-thread in focus" and "horizontal grating in focus"[(2)]. Colouring of the image is caused by natural dispersion of light in the brine[(2)]. Diameter of view field is 23 cm. One half-stroke motion produces internal waves and central vortex only in the lower hemi-space. Thin curved lines above the disk are traces past ascending gas bubbles separated from the disk surface. Thin conical interface is formed directly inside the fluid and gradually retransformed in the mushroom-like vortex below the disk. Full stroke produces internal waves occupying the whole space and autocumulative jet that is mushroom-like vortex below the disk[(3)]. Autocumulative jet is formed inside the fluid and moves towards the disk. It's tip acts as an additional instantaneous source of transient internal waves. Images of disk edge induced vortices are similar to downstream vortices past moving strip[(4)].

References : (1) Heinzel, V. et al., J. of Visualization, 10-1 (2007), 9. (2) Chashechkin, Yu. D., J. of Visualization, 1-4 (1999), 345-354. (3) Chashechkin, Yu. D. and Levitskiy, V. V., J. of Visualization, 6-1 (2003), 59-65. (4) Chashechkin, Yu. D. and Mitkin, V. V., J. of Visualization, 7-2 (2004), 127-134.

Portfolio Paper

Application of Anaglyph Stereo Visualization Technique Using Depth Information

Matsuura, F.*[1] and Fujisawa, N.*[2]

*1 Graduate School of Science and Technology, Niigata University, 2-8050 Ikarashi, Nishi-ku, Niigata 950-2181, Japan. E-mail: mat@xfer.in

*2 Visualization Research Center, Department of Mechanical Engineering, Niigata University, 2-8050 Ikarashi, Nishi-ku, Niigata 950-2181, Japan.

Received 17 October 2007 and Revised 14 November 2007

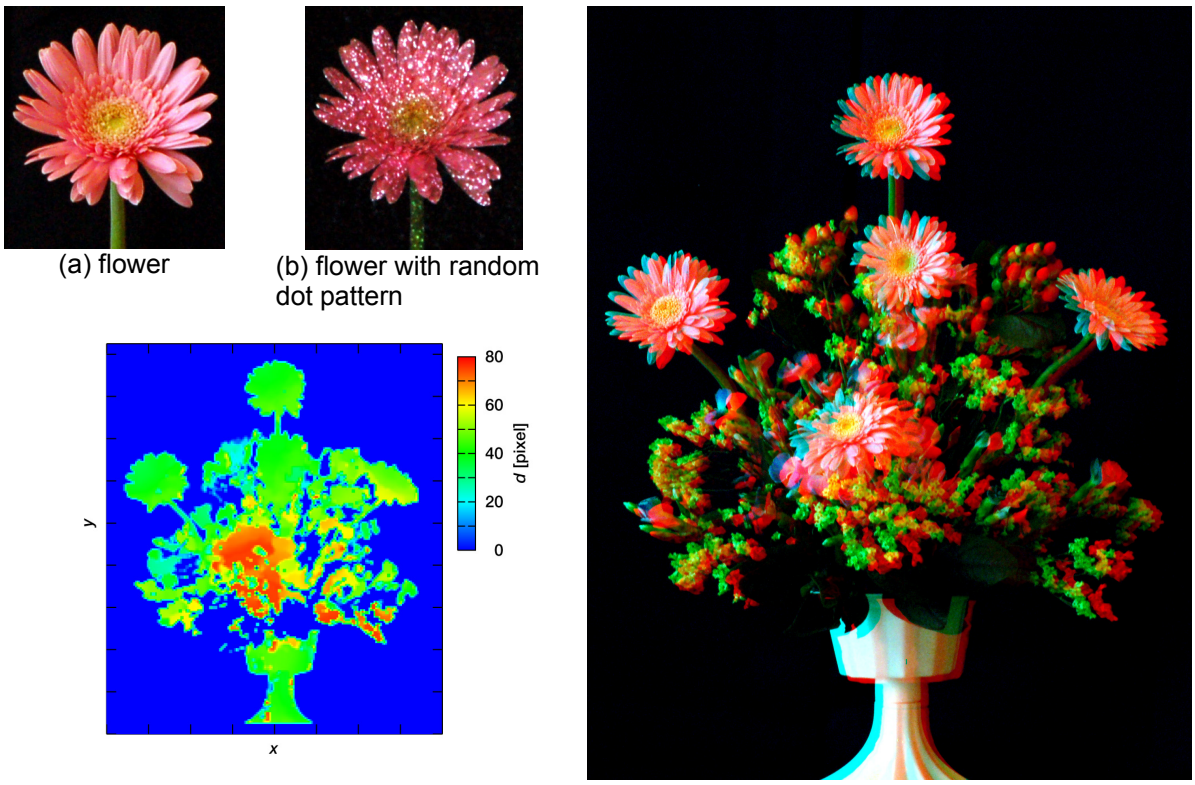

Fig. 1. Anaglyph stereo visualization of flower arrangement using depth information.

This portfolio paper demonstrates the anaglyph stereo visualization technique using depth information(1), which allows 3D visualization of target object by commercial digital color cameras in parallel placement with a certain distance. This technique is applicable to the generation of highly brilliant stereo color images of scientific art(2), (3) with reasonable cost in comparison with the standard method(4). The figures show the procedure of anaglyph stereo imaging and the generated color anaglyph, which is a target object of flower arrangement in white light illumination (a), that in a random dot pattern illuminated by a LCD projector (b), the depth information analyzed by correlation-based-template-matching analysis (c) and the anaglyph stereo image generated by this method (d). The spatial resolution of anaglyph stereo image is high enough (3008 x 2000 pixels) to reproduce well the brilliance of flower arrangement, which is designed by S. Fujisawa and J. Endo. The 3D image of color anaglyph can be seen through red-cyan glasses.

References : (1) Matsuura, F. and Fujisawa, N., Journal of Visualization, 11-1 (2008), 79-86. (2) Bruno, F. et al., Journal of Visualization, 9-3 (2006), 319-329. (3) Fujisawa, N. et al., Journal of Visualization, 10-2 (2007), 163-170. (4) Ideses, I. and Yaroslavsky, L., Journal of Optics A.: Pure and Applied Optics, 7 (2005), 755-762.

Journal of Visualization, Vol. 11, No. 1 (2008) 8

Portfolio Paper

Cowl Opening

Zibarov, A. V.*, Karpov, A. N.*, Medvedev, A. V.*, Elesin, V. V.*, Orlov, D. A.* and Komarov, I. Y.*
* GDT Software Group, Tula, Russia. E-mail: info@cfd.ru ; URL: www.cfd.ru
Received 7 June 2006 and Revised 15 November 2007

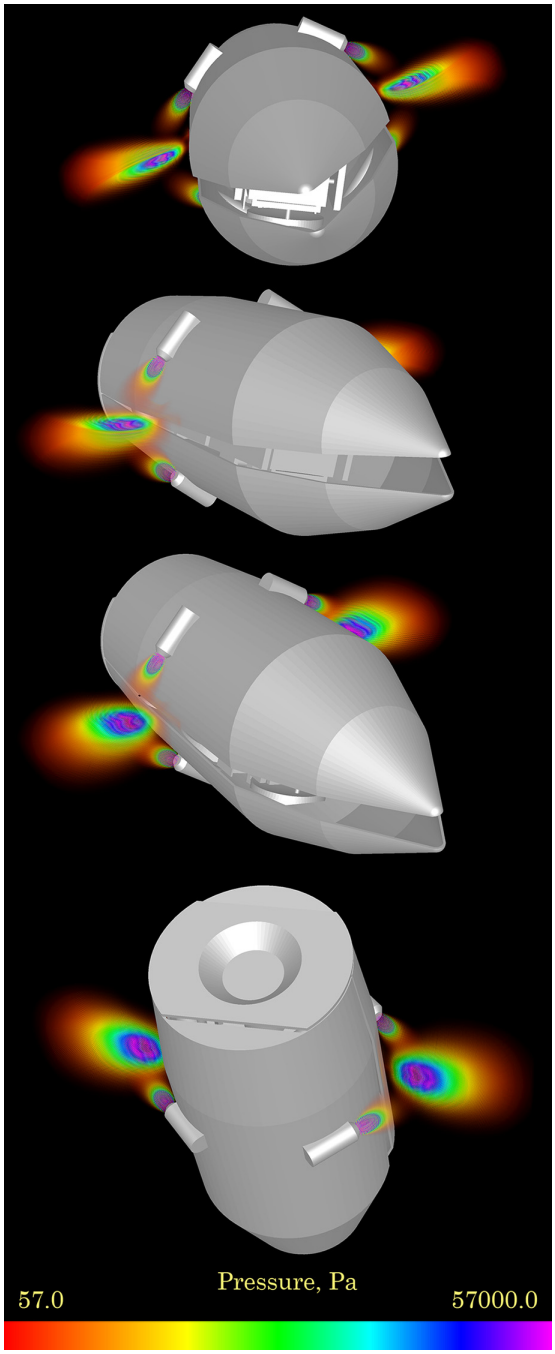

Fig. 1. Pilot engines jet interacting. Pressure distribution.

The force exposure definition problem on a space vehicle at the moment of its opening to output a satellite (Fig. 1) was simulated using the GasDynamicsTool CFD package and the ScientificVR® package provided the visualization.

The pilot engines to open the cowl lids are installed at the direction towards to each other. As a result, when the cowl lids are opened, the satellite is exposed by the air stream, produced by the tractive force of the pilot engines working, and the air stream of the jets interacting. This can lead to the satellite displacement and further trajectory removal.

The velocity force of the air stream springing the cowl up at the height of its opening can be disregarded, as it is essentially lower than the velocity force of the jets from the pilot engines working[1, 2].

The visualization of the pressure distribution through the air stream was performed using the semitransparent voxel technology[3].

On the images presented the pressure range is limited (57 – 57000 Pa) in order to show the process of the jet interaction. It can be enlarged, if there is a necessity to show the whole process of a gas current.

The voxels are colored according to a pressure value. The red color is for low values, and the violet color is for the high ones.

References : (1) Okhitin, V. N. et al., Combustion of Energetic Materials, (2002), 1072-1089. (2) Thiagarajan, V. et al., J. of Visualization, 9-1 (2006), 91-100. (3) Bruno, F. et al., J. of Visualization, 9-3 (2006), 319-330.